# An improved laser-based method and system for measuring web thickness of microdrills considering runout compensation

**Wen-Tung Chang[1,#], Shui-Fa Chuang[1], De-Yi Hong[2], Yi-Shan Tsai[2], Yeong-Shin Tarng[2], Geo-Ry Tang[2] and Fang-Jung Shiou[2]**

1 Opto-Mechatronics Technology Center, National Taiwan University of Science and Technology, Taipei 10607, Taiwan
2 Department of Mechanical Engineering, National Taiwan University of Science and Technology, Taipei 10607, Taiwan
# Corresponding Author / E-mail: wtchang@mail.ntust.edu.tw, TEL: +886-2-2730-1123, FAX: +886-2-2730-1143

KEYWORDS: Microdrill, Web thickness measurement, Laser micro-gauge, Surface scanning laser confocal displacement meter, Runout compensation

*In this paper, an improved laser-based method and system for measuring web thickness of microdrills considering runout compensation is introduced. The improved method is based on the use of a laser micro-gauge (LMG) and a surface scanning laser confocal displacement meter (LCDM). The LMG is used to determine the runout amount and the cross-sectional outer diameter of the microdrill, and the surface scanning LCDM is used to scan the cross-sectional profile of the microdrill to further determine its dual cross-sectional flute depths with runout-related deviation amounts being excluded. Then, the cross-sectional web thickness of the microdrill is calculated through the difference between the determined cross-sectional outer diameter and dual cross-sectional flute depths. An improved laser-based measuring system, for implementing the improved method, was constructed. Experiments meant to measure web thickness of microdrill samples were conducted. It showed that the improved method could achieve better repeatability and accuracy than those achieved by the previous method proposed by Chuang et. al [8]. Also, the measuring results obtained by using the improved method showed good agreement with those obtained by using the traditional destructive measuring method. The improved method and system had been validated feasible for the runout compensation of the web thickness measurement for certain microdrills.*

Manuscript received: January XX, 2011 / Accepted: January XX, 2011

## 1. Introduction

Microdrills, being of nominal diameters ranging between 0.05 and 0.45 mm [1, 2], have been used to produce tiny holes in printed circuit boards. To achieve mass production of microdrills with high and stable quality ensured, superior design, precision manufacturing and inspection techniques must be involved. The drill body of a microdrill can be functionally partitioned into the drill point and the helical flutes. During the drilling process, cutting action inside the workpiece occurs at the drill point, and the helical flutes provide space for chip removal through the screw action. The web of a microdrill is defined as the residual core portion of the drill body without fluted, and the web thickness conflicts with the flute size (i.e., the flute depth). The web thickness is therefore a key parameter to evaluate the rigidity and chip-removal ability of a microdrill. For microdrill manufacturers, the inspection of drill point defects and the measurement of web thickness are quite important to ensure quality control of microdrill products.

So far, some noncontact inspection technologies for microdrills have been developed and possibly applied in the production line. Tien et al. [3], Su et al. [4], and Huang et al. [5] have developed machine vision systems, respectively, to inspect several types of drill point defects and wear of microdrills. Perng et al. [6] have proposed an automated optical inspection system to measure diameters and lengths of microdrills. Huang et al. [7] have employed a laser inspection system to measure diameters and runout phenomena of microdrills.

Recently, Chuang et al. [8] have proposed a laser-based web thickness measuring method and system through the use of the laser micro-gauge (LMG) [9] and the laser confocal displacement meter (LCDM) [10]. Such a web thickness measuring method and system provides potential advantage of replacing a traditional destructive means of the web thickness measurement. (In the traditional method, the drill body of a microdrill to be measured is ground axially from the drill tip to a specified axial location by using a microdrill grinder to yield a ground cross-sectional plane of the drill body. Then, experienced inspectors use a measuring microscope to measure the cross-sectional web thickness at the ground plane.) However, without considering runout phenomena of microdrills, their proposed laser-based measuring system was sometimes not able to achieve sufficient repeatability or accuracy. Therefore, in this paper, an improved laser-based method and system, based on the use of a LMG and a surface scanning LCDM [11], is introduced for the measurement of web thickness considering runout compensation. Experiments meant to measure web thickness of microdrill samples were conducted to test the feasibility of the improved laser-based method and system.

## 2. The Improved Laser-Based Measuring Method

As referred to the cross-sectional profile of a typical microdrill shown in Fig. 1, in which, the cross-sectional web thickness, $w$, is theoretically identical to $D_t$, the diameter of an external common tangent circle $C_t$ of the two cross-sectional flute contours $\Pi_f$s. The two common tangent points are located at points $P_{t1}$ and $P_{t2}$, respectively, and the common tangent circle $C_t$ is centered at point $O_a$, the geometric center (i.e., the axial reference point) of the drill at the cross-sectional plane. Theoretically, the minimum bounding circle $C_b$ of the cross-section of the microdrill overlaps the two cross-sectional margin contours $\Pi_m$s (i.e., the circular-arc contours), and whose diameter, $D_b$, is the cross-sectional outer diameter of the microdrill. Also, the two circles $C_b$ and $C_t$ are concentric. The flute depth $d_{f1}$ (or $d_{f2}$) is the radial distance from point $P_{t1}$ (or $P_{t2}$) outward to the circumference of circle $C_b$. If the diameter of the minimum bounding circle, $D_b$, and the dual cross-sectional flute depths, $d_{f1}$ and $d_{f2}$, are known, the cross-sectional web thickness, $w$, can be calculated by

$$w = D_t = P_{t1}P_{t2} = D_b - (d_{f1} + d_{f2}) \tag{1}$$

According to the measuring principle proposed by Chuang et al. [8], a LMG is used to measure the cross-sectional outer diameter of the microdrill, $D_b$, and a LCDM is used to measure the dual cross-sectional flute depths of the same microdrill, $d_{f1}$ and $d_{f2}$. The cross-sectional web thickness, $w$, is then calculated by using Eq. (1). However, when runout phenomena of microdrills exist, their proposed measuring principle may not have sufficient accuracy to determine the web thickness and needs some improvements.

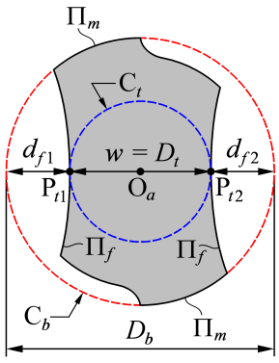


Fig. 1 Cross-sectional geometric characteristics of a typical microdrill

Figure 2(a) shows the schematic diagram of a normal microdrill, in which, the drill body is exaggerated for clarity of illustration. In the figure, a Cartesian coordinate system $O_s$-XYZ is fixed on the frame of a spindle chuck (not shown in the figure) used for holding and rotating the microdrill, while the Z-axis passes through the central axis (i.e., the rotation axis) of the microdrill. The length of the drill body, $l_d$, is defined as the length between the drill tip and a reference point $O_{a0}$. The reference point $O_{a0}$ is the geometric center of the cross-sectional profile of the root of the drill body. At the same time, point $O_{a0}$ is concentric with an axial rorating certer $O_{r0}$ located at the central axis. For any specified cross-sectional profile of the drill body normal to the Z-axis, its axial location, $l_c$, is count from the drill tip to its cross-sectional geometric center $O_a$, while point $O_a$ is also concentric with an axial rorating certer $O_r$ located at the central axis. However, for an abnormal microdrill with runout phenomenon as shown in Fig. 2(b), the abovementioned geometrric correlations may change. When runout phenomenon exists, the drill body will deviate from the central axis of the microdrill. That is, a radial offset $e_0$ may exist between points $O_{a0}$ and $O_{r0}$, and an inclined angle $\alpha$ may also exist between the central line of the drill body and the central axis. Then, the drill tip will have a projection point $O_t$ on the central axis. For this case, the axial location of any specified cross-sectional profile of the drill body normal to the Z-axis, $l_c$, is count from point $O_t$ to an axial rorating certer $O_r$ located at the central axis, while point $O_r$ is a projection point of point $O_a$ located at the central line of the drill body. Thus, the radial offset $e$ [$= l_d\sin(\alpha) - l_c\tan(\alpha) + e_0$] between points $O_a$ and $O_r$ is the eccentric amount of the specified cross-sectional profile, and the subtending angle $\theta$, which is measured counterclockwise from a reference line paralleling the X-axis to line $O_rO_a$, is defined as the rotation angle of the specified cross-sectional profile. The maginitude of $2e$ is the runout amount of the specified cross-sectional profile.

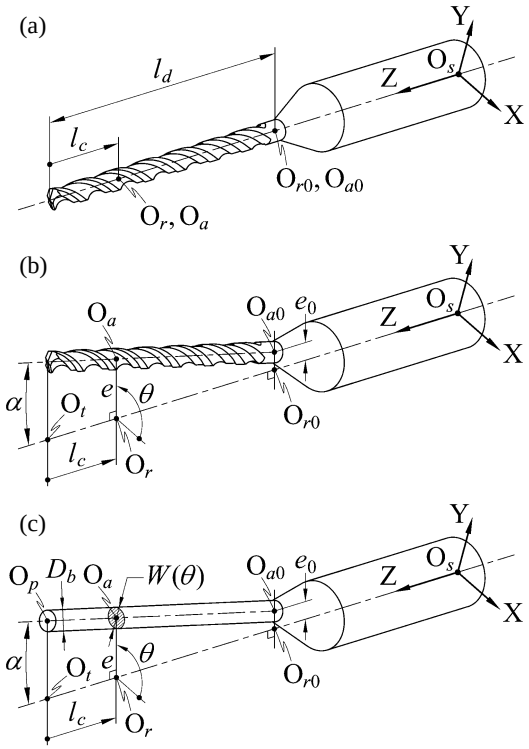


Fig. 2 Schematic diagrams of microdrills: (a) a normal microdrill, (b) an abnormal microdrill with runout phenomenon, and (c) an unmachined workpiece of a microdrill with runout phenomenon

It must be noted that, in Fig. 2(b), the shape of the cross-sectional profile normal to the Z-axis will be slightly different from that normal to the central line of the drill body. Such a situation can be illustrated by using Fig. 2(c), which shows an unmachined workpiece of a microdrill with runout phenomenon. In the figure, point $O_p$ is the center of the end face profile of a round bar and will be the drill tip after machined. The shape of the cross-sectional profile centered at point $O_a$ and normal to the Z-axis is an ellipse, rather than a circle. The width $W(\theta)$ of the cross-sectional ellipse measured along the Y-axis may thus slightly differ from the outer diameter of the round bar, $D_b$. Considering an extreme case that the width $W$ equals to the major axis length of the cross-sectional ellipse, i.e., $W = D_b\sec(\alpha)$, and $D_b$ = 0.35 mm, $O_pO_{a0} = l_d$ = 6 mm, $O_tO_p$ = 15 μm and $e_0$ = 0 μm are given in this case, the magnitude of $\alpha$ is merely 0.1432° [$\sec(0.1432°)$ = 1.00000313 ≈ 1] and thus $W \approx D_b$ = 0.35 mm. In other words, such a slight shape deviation of the cross-sectional profile on influencing the web thickness measurement can be ignored.

In the following sub-sections, the improved measuring method, based on determining the runout amount and the cross-sectional outer diameter with the use of a LMG and determining the cross-sectional flute depths with the use of a surface scanning LCDM, is introduced.

### 2.1 Determination of the Runout Amount and the Cross-Sectional Outer Diameter

Figure 3 shows the illustration of determining the runout amount and measuring the cross-sectional outer diameter of a microdrill by using a LMG. The LMG unit, also known as the scanning laser device [12], basically consists of a transmitting and a receiving parts. As shown in Fig. 3(a), the transmitting part emits a series of parallel laser beams to the receiving part, and the area occupied by the parallel laser beams forms a measuring plane of the LMG unit. A microdrill to be measured is placed between the transmitting and receiving parts with its central axis perpendicular to the measuring plane. When the drill body blocks some of the laser beams emitted, the photodetector in the receiving part can then detect the amount of signals blocked, and an embedded signal processor in the LMG unit can calculate the instantaneous cross-sectional width of the drill body, $W$, in the laser transmission path. At the same time, the signals that are not blocked can also be detected and calculated to obtain the magnitudes of the instantaneous upper and lower gaps, $G_u$ and $G_l$, respectively. The upper and lower gaps are the shortest distances (along the Y-direction) between the cross-sectional profile of the drill body and the upper and lower boundaries of the parallel laser beams [i.e., the boundary lines $\Gamma_u$ and $\Gamma_l$ shown in Fig. 3(b)], respectively. As shown in Fig. 3(b), when the cross-sectional profile is located at an angular position of $\theta$, the magnitudes of $W(\theta)$, $G_u(\theta)$ and $G_l(\theta)$ are detected. Then, when the cross-sectional profile counterclockwise rotates a half cycle to be located at another angular position of $\theta'$ (i.e., $\theta' = \theta + 180°$), the geometric center $O_a$ is shiftted to $O'_a$, and the magnitudes of $W(\theta')$, $G_u(\theta')$ and $G_l(\theta')$ are also detected. Based on rigid body kinematics, $\Delta G_u(\theta)$ and $\Delta G_l(\theta)$ (the differences between magnitudes of gaps) can be calculated by

$$\Delta G_u(\theta) = G_u(\theta') - G_u(\theta) = e[\sin(\theta) - \sin(\theta')] = 2e\sin\theta \quad (2)$$

$$\Delta G_l(\theta) = G_l(\theta') - G_l(\theta) = e[\sin(\theta') - \sin(\theta)] = -2e\sin\theta \quad (3)$$

It must be noted that in the beginning of the measurement, the values of the eccentric amount $e$ and the rotation angle $\theta$ are undetermined. Instead, the angular position of a motor (used for driving the spindle chuck), $s$, can be known through a rotary encoder or step counts. Thus, let the microdrill rotate 1.5 cycles and $s$ be the independent variable, two complete functions of $\Delta G_u(\theta(s))$ and $\Delta G_l(\theta(s))$, which reveal sinusoidal waves, can be ontained by

$$\begin{aligned}\Delta G_u(\theta(s)) &= G_u(\theta'(s)) - G_u(\theta(s)) \\ &= e[\sin(s + s_0) - \sin(s' + s_0)] = 2e\sin(s + s_0)\end{aligned} \quad (4)$$

$$\begin{aligned}\Delta G_l(\theta(s)) &= G_l(\theta'(s)) - G_l(\theta(s)) \\ &= e[\sin(s' + s_0) - \sin(s + s_0)] = -2e\sin(s + s_0)\end{aligned} \quad (5)$$

where $s' = s + 180°$ and $s_0$ is a constant phase difference. In practice, after the measurement, discrete point data of $\Delta G_u$ and $\Delta G_l$ can be obtained. These data should be further processed by using a least-squares sine-fitting approach [13] to find their corresponding fitted functions. Then, the amplitude of the fitted function of $\Delta G_u(\theta(s))$ [or $\Delta G_l(\theta(s))$] is regarded as the runout amount $2e$, and the correlation of $\theta(s) = s + s_0$ can be accordingly determined. After $\theta(s)$ has been determined, the extreme cross-sectional widths of the drill body, $W(\theta_1) = W_{max}$ and $W(\theta_2) = W_{min}$, can also be obtained, respectively, as shown in Fig. 3(c). The diameter of the minimum bounding circle, $D_b$, is thus obtained by

$$D_b = W(\theta_1) = W_{max} \quad (6)$$

which means that the value of the maximum cross-sectional width, $W_{max}$, measured when the cross-sectional profile is located at an angular position of $\theta_1$, is regarded as the cross-sectional outer diameter of the microdrill.

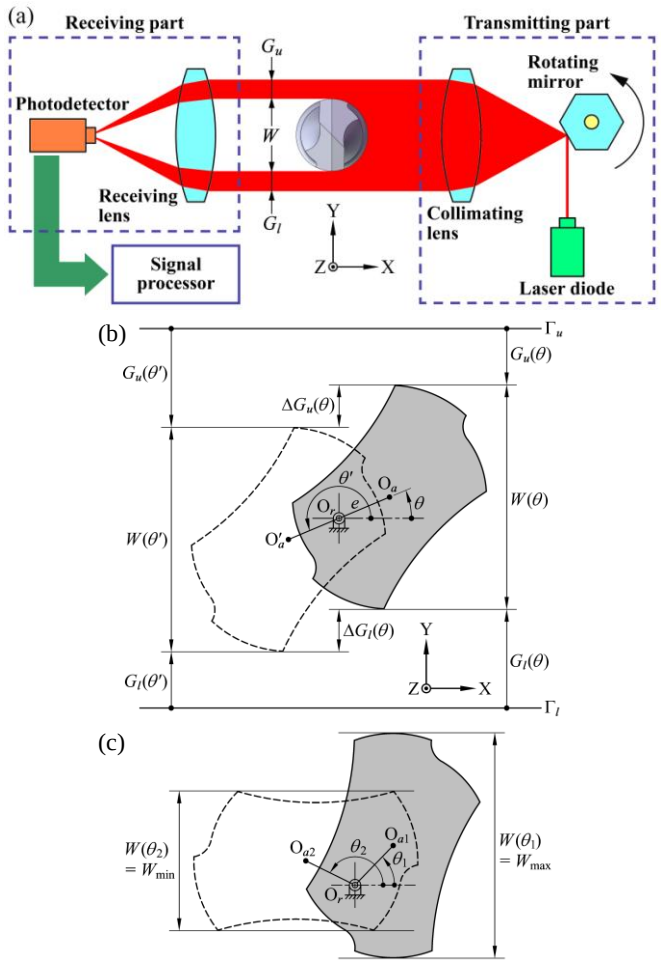


Fig. 3 Illustration of determining the runout amount and measuring the cross-sectional outer diameter of a microdrill by using a LMG

### 2.2 Determination of the Cross-Sectional Flute Depths

Figure 4 shows the illustration of measuring the cross-sectional flute depth of a microdrill by using a surface scanning LCDM. The surface scanning LCDM [11], as compared with the traditional LCDM [10] uesd by Chuang et al. [8], is an advanced distance measuring device based on both the active confocal principle and the reciprocal profile scanning mechanism. As shown in Fig. 4(a), a microdrill to be measured is placed under the LCDM head with the central axis of the drill being perpendicular to the optical axis of the LCDM head. The LCDM head emits a focused laser beam onto the drill body surface through an objective lens that vibrates rapidly up and down (along the Y-direction) by means of a tuning fork unit. The laser beam reflected off the drill body surface is redirected by a half-mirror to an embedded charge-coupled device (CCD) camera for monitoring the location of the laser beam spot. At the same time, the reflected laser beam is also redirected by another half-mirror to converge on a pinhole and then enters a light-receiving element. By

measuring the exact position of the objective lens when the light enters the light-receiving element with sufficient intensity, the distance from the objective lens to the drill body surface can be determined. Furthermore, both the collimating and objective lenses vibrate reciprocally forward and backward (along the X-direction) by means of an oscillating unit to let the emitted laser beam scan the profile of the drill body surface. In other words, when the drill locates at any angular position, multiple distances from the objective lens to the drill body surface can be measured to form a partially-scanned cross-sectional profile. As shown in Fig. 4(b), when the cross-sectional profile is located at an angular position of $\theta_3$, the emitted laser beam scans the profile of the cross-sectional margin (the circular-arc portion) to obtain a set of one-dimensional distance data $d(\theta_3, x)$, in which $x$ is a variable regarding the X-directional position of the emitted laser beam. (It must be noted that when the emitted laser beam cannot touch the target surface or when the inclined angle of the target surface is too large, the LCDM head fails in measuring the distance. Such situations lead to the unmeasurable region shown in the figure.) When the laser beam located at a position of $x_3$ and focused on the highest point $P_3$ at the cross-sectional margin, a locally minimum distance, $d(\theta_3, x_3)$, can be determined. Likewise, as shown in Fig. 4(c), when the cross-sectional profile is located at an angular position of $\theta_4$, the emitted laser beam scans the profile of the cross-sectional flute to obtain a set of one-dimensional distance data $d(\theta_4, x)$. When the laser beam located at a position of $x_4$ and focused on the lowest point $P_4$ at the cross-sectional flute, a locally maximum distance, $d(\theta_4, x_4)$, can be determined. The cross-sectional flute depth, $d_f$, is then obtained by

$$\begin{aligned} d_f &= d(\theta_4, x_4) - d(\theta_3, x_3) - \Delta d \\ &= d(\theta_4, x_4) - d(\theta_3, x_3) - e(\sin\theta_3 - \sin\theta_4) \end{aligned} \tag{7}$$

As seen, the cross-sectional flute depth, $d_f$, is the difference between distances $d(\theta_4, x_4)$ and $d(\theta_3, x_3)$ with a runout-related deviation amount, $\Delta d$, being excluded. However, before Eq. (7) can be applied, the determination of $\theta_3$ and $\theta_4$ must be carried out. In practice, the value of $\theta_3$ should be identical to that of $\theta_1$ (or $\theta_1 + 180°$) shown in Fig. 3(c), and the position of $x_3$ can be accordingly determined. Also, the value of $\theta_4$ should be close to that of $\theta_2$ (or $\theta_2 + 180°$) shown in Fig. 3(c). In order to determine the value of $\theta_4$, let the cross-sectional profile rotate intermittently from $\theta = (\theta_2 - \theta_{c1})$ to $\theta = (\theta_2 + \theta_{c2})$ for $\theta_{c1}$ and $\theta_{c2}$ being specified angular constants, and simultaneously let the LCDM head scan the profile of the cross-sectional flute to obtain a set of two-dimensional distance data $d(\theta, x)$. For each specified angular position of $\theta = \theta_i$, there must be a candidate distance value $d(\theta_i, x_{4c})$ among the one-dimensional data set $d(\theta_i, x)$, where the position of $x_{4c}$ can be determined by

$$x_{4c} = x_3 - e(\cos\theta_3 - \cos\theta_i) \tag{8}$$

Then, for a candidate distance value $d(\theta_i, x_{4c})$ being judged as distance $d(\theta_4, x_4)$, the necessary condition is that its corrsponding focused point $P_i$ should be quite close to the lowest point among all focused points in the one-dimensional data set, and the sufficient condition is that the slope of the focused point $P_i$ (estimated by numerical differences) should be quite close to zero. When at least the necessary condition is satisfied, the value of $\theta_4 \approx \theta_i$, as well as the correlation of $d(\theta_4, x_4) \approx d(\theta_i, x_{4c})$, can be accordingly determined. In addition, after the one-dimensional distance data sets $d(\theta_i, x)$, $d(\theta_3, x)$ and $d(\theta_4, x)$ are measured, they can be processed by using a least-squares polynomial-fitting approach [13] to reduce measuring noise.

Based on the abovementioned method, let the microdrill rotate 1 cycle and the cross-sectional profile be scanned at specified angular positions, the dual cross-sectional flute depths, $d_{f1}$ and $d_{f2}$, can be determined, respectively. After the value of $D_b$ is obtained by using Eq. (6) and those of $d_{f1}$ and $d_{f2}$ are obtained by using Eq. (7), the cross-sectional web thickness, $w$, can be calculated through Eq. (1).

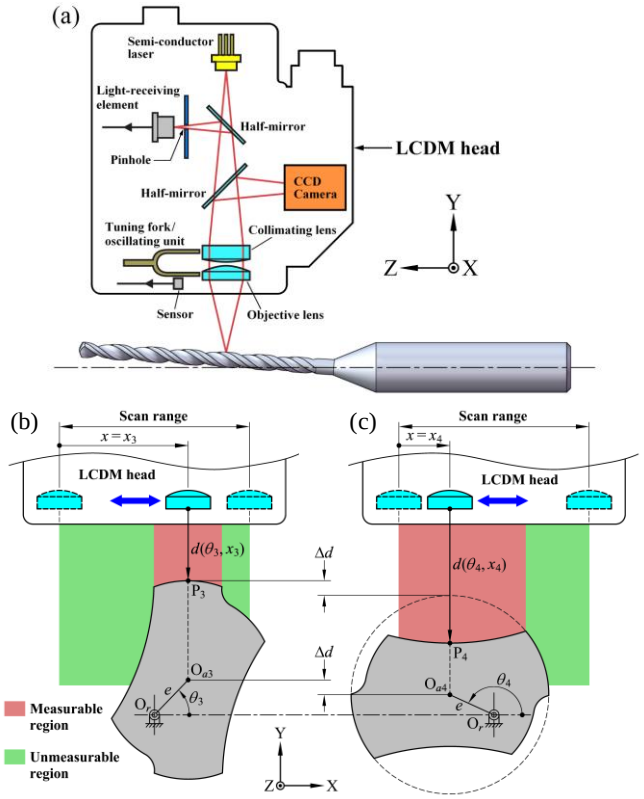


Fig. 4 Illustration of measuring the cross-sectional flute depth of a microdrill by using a surface scanning LCDM

## 3. Setup of the Improved Laser-Based Measuring System

In order to implement the improved measuring method, a laser-based measuring system was constructed, and the setup of which is shown in Fig. 5. The system mainly consisted of a Tokyo Opto-Electronics (TOE) LMG126II LMG unit, a Keyence LT-9011M surface scanning LCDM head, a Nakanishi NR50-5100 ATC rotating spindle chuck carried by a Z-axis linear table, a microdrill tray carried by an X-axis linear table, and an air gripper carried by a Y-axis linear table. The LMG unit, the LCDM head and the Z-axis linear table were all disposed on the same side of a vertical square column, while the X- and Y-axis linear tables were both disposed on a horizontal base plate. The LMG unit (coupled with a TOE LMG-D5-126 LMG controller), whose resolution and accuracy are 0.05 μm and ±1 μm, respectively, was used to determine the runout amount and the cross-sectional outer diameter of a microdrill. The LCDM head (coupled with a Keyence LT-9501H LCDM controller), whose focused laser beam spot is with a diameter of 2 μm and whose resolution and linearity are 0.3 μm and ±0.5% of full scale, respectively, was used to determine the dual cross-sectional flute depths of a microdrill. The rotating spindle chuck (driven by a Mitsubishi HC-KFS43K/MR-J2S-40A servomotor module), whose runout amount is within 1 μm, was used to hold and rotate a microdrill. The air gripper was used to pick a

microdrill from the microdrill tray and then place the microdrill to the rotating spindle chuck, or vise versa. The X- and Y-axis linear tables were respectively driven by two Delta ECMA-C30401ES/ASD-A0121-AB servomotor modules. The Z-axis linear table was driven by a Sanyo Denki 103H548-0410 two-phase stepping motor (coupled with a CSIM CSD204 two-phase stepping driver), and whose reference position was measured by an optical linear encoder that has a resolution of 1 μm for closed-loop motion control. A host computer (not shown in the figure) was prepared for manipulating the motors through an installed National Instruments (NI) PCI-7344 four-axis motion control card, receiving measuring signals from the LMG and LCDM controllers through its RS-232 ports, and switching on/off the spindle chuck and the air gripper through installed relay modules and electromagnetic valves. In order to operate the constructed measuring system through the host computer, human-machine interface software and web thickness measuring programs were developed and integrated in the NI LabView environment.

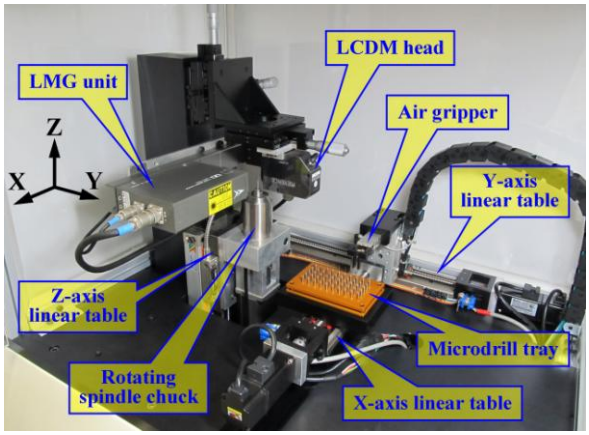

Fig. 5 Setup of the improved laser-based measuring system

Figure 6 shows the measurement of a microdrill sample by using the improved laser-based measuring system. After the Z-axis linear table had carried the microdrill sample to be located at a specified axial position, the microdrill sample rotated 1.5 cycles with a constant angular velocity of 2 rev/min for determining the runout amount and the cross-sectional outer diameter through using the LMG unit. The sampling rate of the LMG was set to be 244 data/cycle for measuring the values of $W(\theta)$ and $G_u(\theta)$. Then, the microdrill sample rotated 1 cycle intermittently to let its cross-sectional profile be scanned at specified angular positions through using the surface scanning LCDM head for determining the dual cross-sectional flute depths. The specified angular positions were in order of $\theta = \theta_1$, $\theta = (\theta_2 - \theta_{c1}) \sim (\theta_2 + \theta_{c2})$ with $\theta_{c1} = \theta_{c2} = 6^\circ$ and an angular interval of 0.2°, $\theta = \theta_1 + 180^\circ$, and $\theta = (\theta_2 + 180^\circ - \theta_{c1}) \sim (\theta_2 + 180^\circ + \theta_{c2})$ with $\theta_{c1} = \theta_{c2} = 6^\circ$ and an angular interval of 0.2°. For each scan, 60 data of measured distances $d(\theta_i, x)$ within a scan range of 120 μm were obtained. The cross-sectional web thickness of the microdrill sample could be accordingly calculated and stored by the host computer. The Z-axis linear table would further carried the microdrill sample to be located at other specified axial positions for performing the measurement.

In addition, for comparison purpose, the function of the reciprocal profile scanning mechanism of the surface scanning LCDM head was set to be closed (i.e., the scan range was set to be zero) in order to implement the measuring principle of the previous method [8]. That is, the microdrill sample rotated 1 cycle with a constant angular velocity of 2 rev/min for measuring a set of distance data $d(\theta)$ through using the LCDM head. Then, two sets of locally maximum and minimum distances among the measured distances $d(\theta)$ were found out to estimate the dual cross-sectional flute depths by calculating their differences without excluding their runout-related deviation amounts.

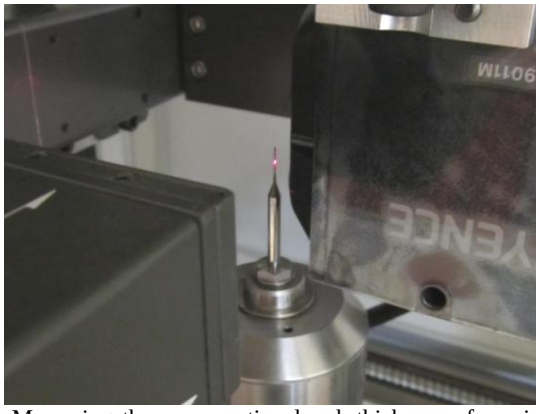
Fig. 6 Measuring the cross-sectional web thickness of a microdrill sample by using the improved laser-based measuring system

## 4. Experimental Results and Discussion

In order to test the feasibility of the improved laser-based method and system, two different experiments meant to measure the web thickness of certain Topoint ST type microdrill samples with a nominal diameter of 0.35 mm were conducted.

In the first experiment, a microdrill sample was repeatedly measured at a specified axial location of $l_c$ = 1.2 mm for 10 times with both the improved method and the previous method [8] being applied. Then, the destructive measuring method was applied to the same microdrill sample for comparison purpose. That is, through using a microdrill grinder, this microdrill sample was ground axially to the specified location of $l_c$ = 1.2 mm to yield a ground cross-sectional plane, and a Mitutoyo MF-510TH measuring microscope was used to repeatedly measure the cross-sectional web thickness at the ground plane for 10 times, as shown in Fig. 7. Table 1 shows the results of this experiment. As can be seen, for the improved method, the mean measured value and repeatability (based on the well-known three-standard-deviation-band approach) of the cross-sectional web thickness were 0.1470 mm and ±0.96 μm, respectively, while those for the previous method [8] were 0.1433 mm and ±2.48 μm, respectively. As a result, the repeatability of the improved method was merely 38.7% of that of the previous method [8]. Also, considering a mean runout amount of 28.724 μm, the relative difference between the mean measured web thickness values obtained by using the improved method and the destructive measuring method was merely 0.5 μm, about 1.7% of the mean runout amount; while that between the previous method [8] and the destructive measuring method was 3.2 μm, about 11.1% of the mean runout amount.

The second experiment, as a measuring case study, was conducted by repeatedly measuring a microdrill sample at four specified axial locations of $l_c$ = 1.2, 2.1, 3.0 and 3.9 mm for 5 times with the improved method, the previous method [8] and the destructive measuring method being applied, respectively. Table 2 shows the mean measured values obtained from this experiment. As can be observed, all the relative differences between the mean measured values obtained by using the improved method and the destructive

measuring method were less than 1 μm, while those between the measured values obtained by using the previous method [8] and the destructive measuring method ranged between 3.3 to 3.6 μm. In other words, the measuring results obtained by using the improved method showed good agreement with those obtained by using the destructive measuring method. However, in this case, the previous method [8] was slightly inaccurate for the web thickness measurement.

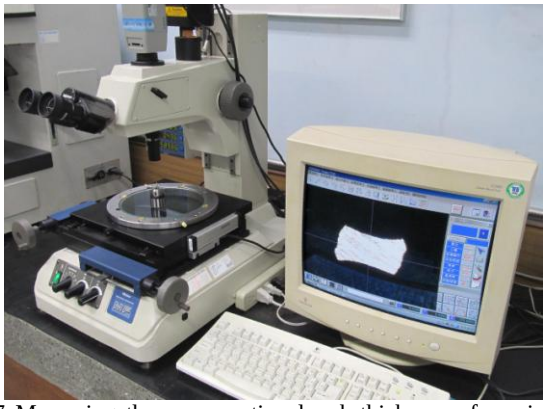

Fig. 7 Measuring the cross-sectional web thickness of a microdrill sample by using a measuring microscope (based on the traditional destructive measuring method)

Table 1 Results of the first experiment

| | Outer diameter $D_b$ (mm) | Runout amount $2e$ (μm) | Web thickness $w$ (mm) | | |
|---|---|---|---|---|---|
| | | | Improved method | Previous method [8] | Destructive measuring method |
| Measurement #1 | 0.3437 | 28.726 | 0.1468 | 0.1428 | 0.1462 |
| Measurement #2 | 0.3437 | 28.749 | 0.1471 | 0.1431 | 0.1466 |
| Measurement #3 | 0.3437 | 28.726 | 0.1466 | 0.1439 | 0.1472 |
| Measurement #4 | 0.3433 | 28.726 | 0.1469 | 0.1421 | 0.1467 |
| Measurement #5 | 0.3434 | 28.718 | 0.1472 | 0.1441 | 0.1458 |
| Measurement #6 | 0.3434 | 28.706 | 0.1475 | 0.1443 | 0.1476 |
| Measurement #7 | 0.3435 | 28.714 | 0.1466 | 0.1427 | 0.1459 |
| Measurement #8 | 0.3437 | 28.661 | 0.1469 | 0.1425 | 0.1464 |
| Measurement #9 | 0.3437 | 28.764 | 0.1473 | 0.1434 | 0.1470 |
| Measurement #10 | 0.3437 | 28.749 | 0.1474 | 0.1445 | 0.1460 |
| Mean value | 0.3436 | 28.724 | 0.1470 | 0.1433 | 0.1465 |
| Standard deviation | 0.00016 | 0.0285 | 0.00032 | 0.00083 | 0.00059 |
| Repeatability | ±0.00049 | ±0.0854 | ±0.00096 | ±0.00248 | ±0.00178 |

Table 2 Results of the second experiment

| Specified axial location $l_c$ (mm) | Outer diameter $D_b$ (mm) | Runout amount $2e$ (μm) | Web thickness $w$ (mm) | | |
|---|---|---|---|---|---|
| | | | Improved method | Previous method [8] | Destructive measuring method |
| 1.2 | 0.3434 | 28.716 | 0.1471 | 0.1431 | 0.1467 |
| 2.1 | 0.3420 | 26.820 | 0.1665 | 0.1625 | 0.1659 |
| 3.0 | 0.3427 | 26.006 | 0.1880 | 0.1842 | 0.1875 |
| 3.9 | 0.3398 | 20.152 | 0.2036 | 0.1995 | 0.2029 |

## 5. Conclusions

An improved laser-based method and system for measuring web thickness of microdrills, based on the use of a LMG and a surface scanning LCDM, has been introduced in this paper. In the improved method, the LMG is used to determine the runout amount and the cross-sectional outer diameter of the microdrill, and the LCDM is used to scan the cross-sectional profile of the microdrill to further determine its dual cross-sectional flute depths with runout-related deviation amounts being excluded. Then, the cross-sectional web thickness of the microdrill can be calculated through the difference between the determined cross-sectional outer diameter and dual cross-sectional flute depths. A laser-based measuring system had been constructed in order to verify the feasibility of the improved method. Experiments meant to measure web thickness of microdrill samples with a nominal diameter of 0.35 mm had been conducted. The experimental results showed that the improved method could achieve a repeatability of ±1 μm, which was about 40% of that achieved by using the previous method [8]. Also, the relative differences between the mean measured values of the cross-sectional web thickness obtained by using the improved method and the traditional destructive measuring method were less than 1 μm, while those between the mean measured values obtained by using the previous method [8] and the traditional destructive measuring method were about 3 to 4 μm. In conclusion, the improved laser-based method, combined with the constructed measuring system, had been validated an accurate and feasible means for the runout compensation of the web thickness measurement for certain microdrills.

## REFERENCES


1. Topoint Technology Corp., available at http://www.topoint.tw/en/index.htm.
2. Tera Autotech Corp., available at http://www.teraauto.com.tw/english/main.php.
3. Tien, F. C., Yeh, C. H. and Hsieh, K. H., "Automated Visual Inspection for Microdrills in Printed Circuit Board Production," Int. J. Prod. Res., Vol. 42, No. 12, pp. 2477-2495, 2004.
4. Su, J. C., Huang, C. K. and Tarng, Y. S., "An Automated Flank Wear Measurement of Microdrills Using Machine Vision," J. Mater. Process. Technol., Vol. 180, No. 1-3, pp. 328-335, 2006.
5. Huang, C. K., Liao, C. W., Huang, A. P. and Tarng, Y. S., "An Automatic Optical Inspection of Drill Point Defects for Micro-Drilling," Int. J. Adv. Manuf. Technol., Vol. 37, No. 11-12, pp. 1133-1145, 2008.
6. Perng, D. B., Hung, C. Y. and Chen, Y. C., "An AOI System for Microdrill Measurement," Proc. 18th Int. Conf. Prod. Res., Salerno, Italy, 2005.
7. Huang, C. K., Wang, L. G., Tang, H. C. and Tarng, Y. S., "Automatic Laser Inspection of Outer Diameter, Run-Out and Taper of Micro-Drills," J. Mater. Process. Technol., Vol. 171, No. 2, pp. 306-313, 2006.
8. Chuang, S. F., Chen, Y. C., Chang, W. T., Lin, C. C. and Tarng, Y. S., "Nondestructive Web Thickness Measurement of Micro-Drills with an Integrated Laser Inspection System," Nondestruct. Test. Eval., Vol. 25, No. 3, pp. 249-266, 2010.
9. Tokyo Opto-Electronics Corp., Laser Micro-Gauge, available at http://www.toe.co.jp/lmghome_e.htm.
10. Keyence Corp., Laser Confocal Displacement Meter, available at http://www.keyence.com/dwn/downloadlt_ka.pdf.
11. Keyence Corp., Surface Scanning Laser Confocal Displacement Meter, available at http://www.keyence.com/dwn/lt_9000.pdf.
12. Groover, M. P., Automation, Production Systems, and Computer-Integrated Manufacturing, 2nd edition, Prentice Hall, Upper Saddle River, New Jersey, pp. 745-746, 2001.
13. Hornbeck, R. W., Numerical Methods, Prentice Hall, Upper Saddle River, New Jersey, pp. 121-143, 1982.